Front. Eng. Manag. 2019, 6(1): 62–69
https://doi.org/10.1007/s42524-019-0001-z

RESEARCH ARTICLE

Qian CHEN, Kai ZHENG, Qingtao FAN, Kun WANG, Haiyan YANG, Jianxin JIANG, Shijie LIU

Solvability and thermal response of cellulose with different crystal configurations

Abstract Cellulose is a biodegradable and renewable natural material that it is naturally resistant to breaking and modification. Moreover, the crystalline structure of cellulose is a major factor restricting its industrial utilization. In this study, cellulose polymorphs were prepared from natural cellulose, and their solvability and thermal response were investigated. Using liquid- and solid-state NMR signals, the distinct types and dissolving states of cellulose polymorphs were identified. The thermal behavior of the polymorphic forms of cellulose-d was also evaluated, and cellulose II exhibited the poorest thermal stability and a unique exothermic reaction.

Keywords cellulose, crystal structure, thermal response, XRD, CP/MAS ^{13}C NMR

Received March 6, 2018; accepted April 18, 2018

Qian CHEN, Kai ZHENG, Kun WANG (✉), Jianxin JIANG
Beijing Key Laboratory of Lignocellulosic Chemistry, College of Materials Science and Technology, Beijing Forestry University, Beijing 100083, China
E-mail: wangkun@bjfu.edu.cn

Qingtao FAN
Beijing Institute of Science and Technology Information, Beijing 100044, China

Haiyan YANG
College of Chemical Engineering, Southwest Forestry University, Kunming 650224, China

Shijie LIU
Department of Paper and Bioprocess Engineering, SUNY College of Environmental Science and Forestry, 1 Forestry Drive, Syracuse, NY 13210, USA

This work was funded by the National Natural Science Foundation of China (Grant No. 31770622), the Beijing Natural Science Foundation (Grant No. 6174046), the Fundamental Research Funds for the Central Universities (No. 2017PT13) and the China Scholarship Council (International Clean Energy Talent Programme (iCET), Grant No. 201702660054).

1 Introduction

In recent years, concerns about global climate change, the security and cost of energy supply, and the desire to shift toward a "low carbon" world have raised interest in biofuels as an alternative to conventional fossil fuels. Biofuels could reduce greenhouse gas (GHG) emissions and the dependence on non-renewable fossil fuels, while moving toward a green, low-carbon economy. According to a benchmark scenario projected for 2030, the reduction of CO_2 emissions would reach 43% by adopting various technologies and creating less polluting energy. Lignocellulosic residues are a second-generation and advanced (low-carbon and sustainable) feedstock, different from food biomass (first-generation feedstock), and do not compete for food-related land and resources (Ashraf et al., 2017). Cellulose (around 1.5×10^{12} tons annual) is considered to be the most renewable material, and a desirable natural polymer source in the biobased material and sustainable industries. Cellulose is used in traditional industries such as textiles, papermaking, and plastic, as well as in the food and chemical industries, in addition to fields such as medicine, construction, agriculture, forestry, and biochemistry (Wang et al., 2013). Exploiting the advantages of cellulose can reduce energy consumption, greenhouse gas emission, and the negative influence of agricultural markets and food prices, thus addressing problems such as resource shortages and environmental pollution (Perlack et al., 2005; Wang and Deng, 2009). Thus, the research, development, and utilization of cellulose offer alternative development routes to achieving low-carbon objectives, promoted by technologies and low-pollution energy systems.

Compared with synthetic biodegradable materials, cellulosic materials have many advantages. First, cellulosic materials can be completely degraded by microorganisms, and thus differ from biodegradable materials made by blending biobased materials with polyolefins, which are not biodegradable. Secondly, hydroxyl groups exist on a

cellulose macromolecular chain, which have strong reaction performance and designability. Therefore, cellulose processing technologies are relatively simple, low-cost, and non-polluting. Thirdly, cellulose is non-toxic, which is critical for many applications (Huang et al., 2016). The use of non-toxic and non-polluting organic solvents to spin cellulose into regenerated cellulose has resulted in a breakthrough in the development of the textile industry to a certain extent (Chen et al., 2014). Regenerated cellulose separation membranes are also an important membrane material that can remove heavy metals from polluted water (Madaeni and Heidary, 2011). The abundance of hydroxyl groups in cellulose makes it easy to be modified and synthesized, and allows complete decomposition into carbon dioxide and water by microorganisms without pollution. As a natural polymer material, cellulose microspheres reproducibly degrade and show good biocompatibility, and have been extensively employed as chromatographic stationary phases, adsorbents, and bio-affinity carriers after being highly modified, thus playing an important role in environmental science, separation engineering, and biomedicine (Luo and Zhang, 2010; Wang et al., 2015; Jin et al., 2012). Hydrogel is a highly cross-linked three-dimensional network polymer, capable of adsorbing substantial amounts of solution to establish swell equilibrium without being dissolved, while maintaining the shape and properties of the solid. By introducing chemical or physical action to cellulose chains, biobased hydrogels can exhibit excellent water absorption and water-holding capacities, and are hence useful in the adsorption of heavy metal pollution, drug release, and tissue engineering (Lou et al., 2014; Tsarevsky et al., 2004).

Cellulose is formed by glucose with β-1,4 glycosidic linkages, but the degree of polymerization of cellulose from different sources differs (Zhang et al., 2008). Cellulose is a semi-crystalline natural polymer with a partially crystallized region in which molecular chains are arranged regularly, while regions with irregularly arranged molecular chains form amorphous regions. In the crystalline region, the strong force leads to a regular arrangement of cellulose chains. In the amorphous region, the interaction force of cellulose molecular chains is weak, and the arrangement between them is loose and irregular (Himmel et al., 2007). The cellulose chain is a long molecule chain, passing through multiple crystalline and amorphous regions. The crystalline area of cellulose has a tremendous influence on its physical properties, such as mechanical strength, melting point, and thermal stability. Because the β-1,4 glycosidic bond energies between repeating glucose units are high, it is difficult to completely break the linkages and obtain glucose (Jeoh et al., 2007). In addition, the hydroxyl groups in cellulose chains induce the formation of a three-dimensional network structure. Because of inter- and intra-molecular hydrogen bonds between cellulose chains, the dissolution and modification of cellulose is difficult with common solvents (Chen et al., 2006). Different pretreatment technologies have been shown to ameliorate the subsequent hydrolysis of cellulose by breaking plant cells at a certain degree by altering, moving or solubilizing lignin, breaking the bonds of lignin-carbohydrate complexes (LCC), hydrolyzing a proportion of hemicellulosic moieties, and reducing cellulose crystallinity (Kumar et al., 2009; Mosier et al., 2005). Chemical pretreatments have been extensively investigated, including the use of acids, alkalines, and organosolvents, and novel green technologies for cellulose dissolution are attracting growing interest, given serious environmental pollution and the desire to improve the quality of living environments (Yang and Wyman, 2008). Many kinds of solvent, such as N-methylmorpholine-N-oxide (NMMO) and aqueous NaOH solutions, have been demonstrated to dissolve cellulose (Qin et al., 2013a), and solvents that are environmentally friendly and low-cost are the most important indexes of sustainable chemistry. In particular, the NaOH/urea system has considerable potential in dissolving cellulose and preparing cellulose derivatives (Qin et al., 2013b). Egal et al. found that when precooling an NaOH/water system$\leqslant$0°C, its ability to dissolve microcrystalline cellulose improved, and the optimal concentration range for dissolving cellulose was 7%–10%. A large amount of NaOH was combined with water, not bonded with cellulose, and the dissolution effect was poor as the NaOH concentration was less than 7%. In contrast, the alkalinization of cellulose occurred as the NaOH concentration grew above 10% (Egal et al., 2008). Furthermore, the degree of polymerization of cellulose was strictly required in this system. Further, the addition of urea to the NaOH solvent increased cellulose solubility. When the NaOH/urea mix was pre-cooled, NaOH hydrates associated with cellulose disrupted its internal three-network structure. At the same time, urea was encapsulated by the NaOH hydrate and cellulose conjugates to prevent aggregation (Liebert et al., 2010). In the NaOH/urea/H_2O solution, the dissolving behavior of cellulose was verified to be connected with temperature, the degree of polymerization, molecular weight, and concentration, and the already-formed gels could not be further processed by cooling or heating cycles (Cai et al., 2008). Many factors affect dissolution, such as the pre-cooling temperature of the solvent, dissolution time, and mixing strength. Hence, there is ongoing research for environment-friendly, low-cost anti-cellulose degradation and rapid dissolution.

Normally, cellulose exists naturally through the formation of nanocellulose, and solid-state cellulose has five crystallization variants, cellulose I, II, III, IV, and X). The unit cell of natural cellulose is cellulose I, such that wood, cotton, hemp, and other natural celluloses have a cellulose I structure. Cellulose II is most often obtained from cellulose I after regeneration and mercerization. Furthermore, the transformation from cellulose I to cellulose II can be realized by treating and ball milling it in water. In

cellulose II, hydrogen bonds exist between corrugated sheets formed with opposite-polarity cellulose chains. (Nishino et al., 2004). Cellulose III can be classified into two categories, cellulose III-1 and cellulose III-2, by taking cellulose I and cellulose II as starting materials and adding liquid ammonia or certain amines, respectively (Yui et al., 2010). The transformation between cellulose I and III-1 and that between cellulose II and III-2 are reversible via thermal or chemical treatments (Sarko, 1978). Thermal analyses of cellulose are normally involved in the development of fire-retardant wood and cellulose material, energy resources, and industrial chemicals. The effect of the degree of cellulose crystallinity on the loss of absorbed water on the thermal degradation curve and thermal decomposition of cellulose have been reported (Bertran and Dale, 1986; Junior, 2000). However, the crystal configuration, has not yet been studied. In this investigation, the crystal configuration of microcrystalline cellulose was transformed and then subjected to Fourier transform infrared spectroscopy (FTIR), X-ray diffractometry (XRD), differential thermal analysis (DTA), and nuclear magnetic resonance (NMR) analyses to study the dependence of solvability and thermal stability on the crystallinity of cellulose.

2 Materials and methods

2.1 Materials

Microcrystalline cellulose powder (Avicel PH-101, Sigma-Aldrich, St. Louis, USA) was employed as the original cellulosic sample (cellulose I). Deuterium oxide (D_2O) and sodium deuteroxide (NaOD) (Sigma-Aldrich, St. Louis, USA) were sealed in a glass capillary. All other chemicals and reagents were analytical grade unless otherwise stated.

2.2 Crystal configuration transformation of cellulose

Cellulose II was obtained by steeping the microcrystalline cellulose powder in 15% NaOH at 60°C for 4 h, followed by thorough washing with deionized water. After freeze-drying, cellulose I and cellulose II were soaked in the ethanediamine (EDA) solution (75 wt.%) for 2 h, respectively, and then subjected to successive washing with methanol and water until neutrality was obtained (Ishikawa et al., 1997). Finally, the cellulosic residues with cellulose III-1 and III-2 were separated by configuring and freeze-drying, respectively.

2.3 Characterization of the cellulosic samples

The XRD analysis were performed with an XRD-6000 instrument (Shimadzu, Japan) with Ni-filtered Cu-Kα radiation (v = 1.54 Å), by scanning from 5° to 45° (2θ) with a goniometer at 5°/min. A current of 40 mA and voltage of 40 kV were used. Solid samples were placed on an aluminum holder and the crystallinity (*CrI*) was determined using the following equation (Segal et al., 1959):

$$CrI(\%) = (I_{020} - I_{\mathrm{am}})/I_{020} \times 100$$

I_{020} : intension of the crystalline portion at about $2\theta = 22.5°$

I_{am} : intension of the amorphous portion at about $2\theta = 18°$

FTIR analysis was performed on an FTIR spectrophotometer (Tensor 27, Bruker, Germany) with a KBr disc containing 1% samples. The absorption mode was used to record the spectra, from 1800 to 800 cm^{-1}, and the baseline was corrected using the rubber-band method. Solid ^{13}C (cross polarization/magic angle spinning, CP/MAS) NMR analysis was performed at 75.5 MHz with a Bruker DRX-400 spectrometer (Germany). All cellulosic samples were placed in 7 mm zirconia rotors, then directly scanned according to a CP pulse program with match (1 ms) and delay (2 s) between transients. The liquid-state 1D (^1H) and 2D (heteronuclear single quantum coherence, HSQC) NMR spectra were obtained after completely dissolving the cellulosic samples in a NaOD/Urea/D_2O (7/12/81, wt.%) system at −12.5°C and then measured at room temperature. DTA and thermogravimetric analysis (TGA) of the cellulosic samples were conducted with a simultaneous thermal analyzer (DTG-60, Shimadzu, Japan). A pure nitrogen flow of 30 mL/min was applied as a carrier gas to provide an inert ambient flow and remove gaseous products. The samples weighed approximately 6 mg and were heated from room temperature to 600°C at a heating rate of 10°C/min.

3 Results and discussion

The crystal configuration of cellulose is a critical factor in resisting biodegradation and chemical modification. Therefore, the crystal characteristics of all samples were initially confirmed by powder XRD, which is a reliability index of the cellulose crystal transformation (Fig. 1). Generally, aqueous NaOH can induce a substantial reduction in both cellulose configuration and crystallinity. In this study, an alkaline treatment was applied to the cellulose I sample with a 15% NaOH aqueous solution for 4 h at 60°C to prepare the cellulose II allomorph, shown by the presence of a doublet in the XRD curve for the 10 and 002 peaks, with 2θ = 15.2°, 20.6°, and 22.4° for the (10), (110), and (020) planes in the XRD patterns being characteristic of cellulose I crystals (Fig. 1), and peaks at 2θ = 12.3°, 20.1°, and 21.8° belonging to the crystal planes (10), (110), and (200), respectively, for cellulose II. Clearly, the XRD

pattern of cellulose III-1, with diffraction peaks at 15.2° (10), 20.1° (110), and 22.5° (020), is similar to that of cellulose I, and that of cellulose III-2, with diffraction peaks at 12.3° (10), 19.9° (110), and 21.7° (020) is similar to that of cellulose II. This result is consistent with the conclusion that cellulose I and III-1, and cellulose II and III-2, respectively, belong to the cellulose I and II family (Isogai et al., 1989). Two approaches were used to explain this different family characteristic: the cellulose chains' polarity between the two families differed, and the conformational difference of the cellulose chains was the primary reason while the chain polarities were the same (Langan et al., 1999). Cellulose II possessed the lowest intensity, corresponding to the lowest value of *CrI* (12%). Thus, the EDA treatment led to the formation of intramolecular and intermolecular hydrogen bonds between cellulose chains, but resulted in the transformation of the crystal configuration. The diffraction peaks of different kinds of biomass materials are different, and the positions of primary peaks are closely related to the distance between the hydrogen bonds in cellulose I. The water content and crystallite size in the sample also affect the diffraction peaks (Cheng et al., 2011). By considering the treatment temperature, the variation of cellulose crystal from cellulose I to cellulose II only occurred as the temperature dropped to −15°C, and the gradual transformation of crystal configuration was observed as a function of incubation time (Wang and Deng, 2009). Meanwhile, the regeneration of cellulose also induced an incremental increase of the degree of polymerization, from approximately 300 for the starting viscose rayon to about 540, similar to that of Lyocell (~600) (Cai et al., 2004).

The FTIR spectrum was also used to explore the structural variation of cellulose. The band at 1615 cm^{-1} is associated with the C = O stretching vibration, the absorption peak at 1368 cm^{-1} to C–H symmetric bending, and the peaks around 1227 cm^{-1} and 1140 cm^{-1} are related to the asymmetric extension of carboxylate group and the C–O–C extension of alkyl ether. The sharp band around 890 cm^{-1}, which is ascribed to the C_1 group frequency in ring, is characteristic of the *β*-glycosidic linkage in the glucose units of cellulose (Teng et al., 2016). The peak near 1420 cm^{-1} is associated with the CH_2 scissoring motion, and the intensity was significantly weakened in the cellulose II and cellulose III-2, which was probably related to the breaking of intramolecular hydrogen bonds involving O_6 (Zhang et al., 2002). Additionally, the band near 955 cm^{-1}, which is associated to the carbocycle in cyclic compounds, showed obvious differences between the cellulose I and II families, likely resulting from the difference in cell parameters. Since the O–H region in cellulose II is larger than that in cellulose I, the O–H area increased during the conversion from cellulose I to cellulose II (Moigne and Navard, 2010).

The behavior of the polymorphic forms of cellulose during thermal destruction was also evaluated, and the TGA and DTA signals vs. temperature are shown in Fig. 1. The thermal degradation of cellulose mainly occurs via two types of reactions: a rapid pyrolysis accompanied by levoglucosan formation at higher temperatures, and a

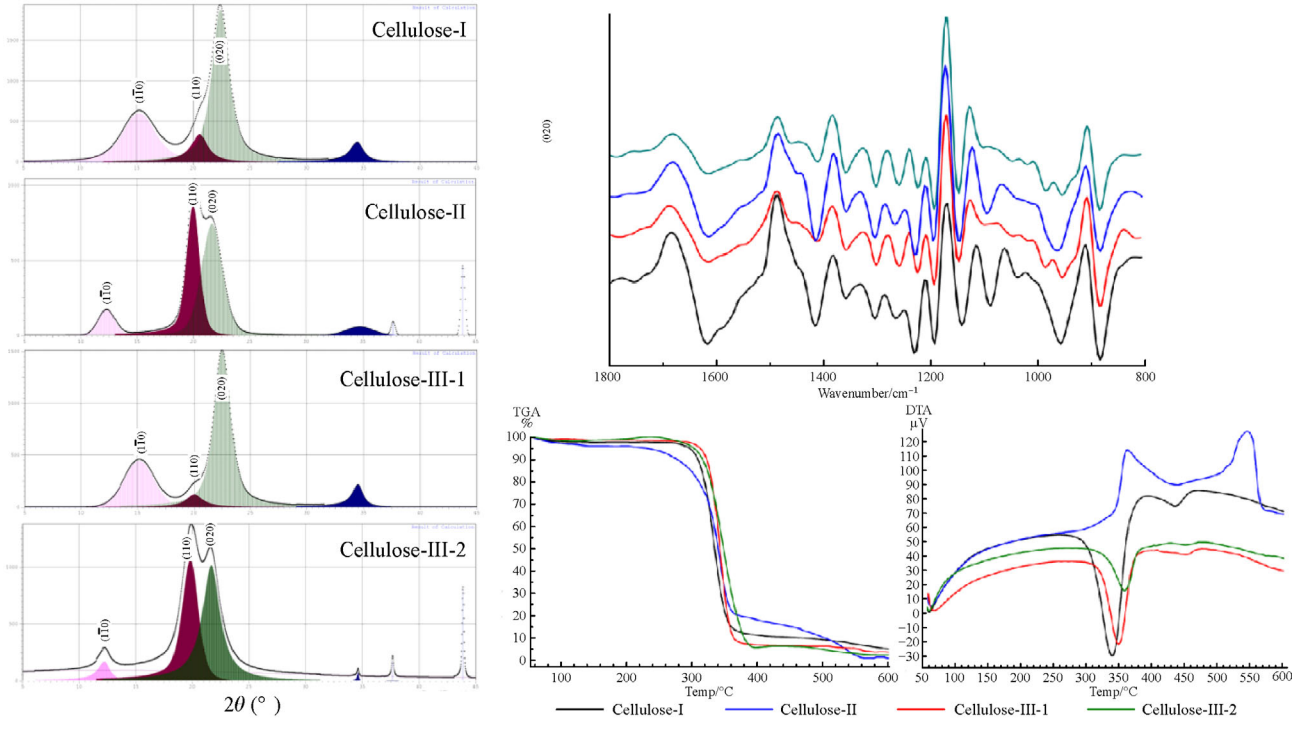

Fig. 1 XRD patterns (left), FTIR (right top), and thermal stability (right bottom) of cellulosic samples

gradual degradation/decomposition with charring at lower temperatures (Balat, 2008). Thermal degradation occurred more rapidly for the sample with more domains and organization levels, which may be explained by its higher weight loss rate at a certain temperature. Curves in the TGA pattern show that a dramatic weight loss in the cellulose samples occurred in the temperature range 260°C–400°C, and the highest weight loss rate was concentrated in the range of 340°C–360°C. As for the weight loss after final pyrolysis, cellulose II exhibited the poorest thermal stability. The initial temperature of cellulose II was near 260°C, which was lower than that of other samples. Furthermore, a second thermal degradation occurred with cellulose II, starting near 450°C. Although this phenomenon was also shown in cellulose III-2, the degree of degradation was limited. It is surprising to note that the exothermic peaks are only present in the DTA curve of cellulose II, and the endothermic peaks of cellulose I, III-1, III-2 were found at 340°C, 360°C, and 350°C, respectively. Cellulose crystallinity has been shown to affect the degradation patterns during thermal analysis, and the initiation of thermal degradation was probably inhibited by stable connections in the crystalline domains of cellulose, including hydrogen bonding, the absence of irregularities, and van der Waals' interactions (sites with higher reactivity) (Junior, 2000).

CP/MAS ^{13}C NMR spectra provided more evidence for the structural transformation of cellulose (Fig. 2). The ^{13}C chemical shifts are given in δ values (ppm) and the peaks in all spectra were assigned based on the literature values (Isogai et al., 1989; Lennholm et al., 1994; Kono et al., 2003; Liitiäet al., 2003; Chen et al., 2015), as follows: cellulose I and III-1: C_1 (105.2 ppm), C_4-amorphous (83.2 ppm), C_4-crystalline (87.6 ppm), C_2, C_3, and C_5 (69.6 to 75.5 ppm), and C_6-amorphous (62.4 ppm), C_6-crystalline (65.5 ppm); cellulose II and III-2: C_1 (106.2 ppm), C_4 (86.1 ppm), C_2, C_3, and C_5 (69.4 to 75.8 ppm), and C_6 (62.7 ppm). Not surprisingly, the cellulose I and II families exhibited remarkable differences in the two carbons, C_4 and C_6, where the broader upfield signal originated from the less-ordered and disordered cellulose chains, while the downfield signal corresponded to the highly ordered crystal structure. This phenomenon was likely associated with the transformation of the t-g conformation in cellulose

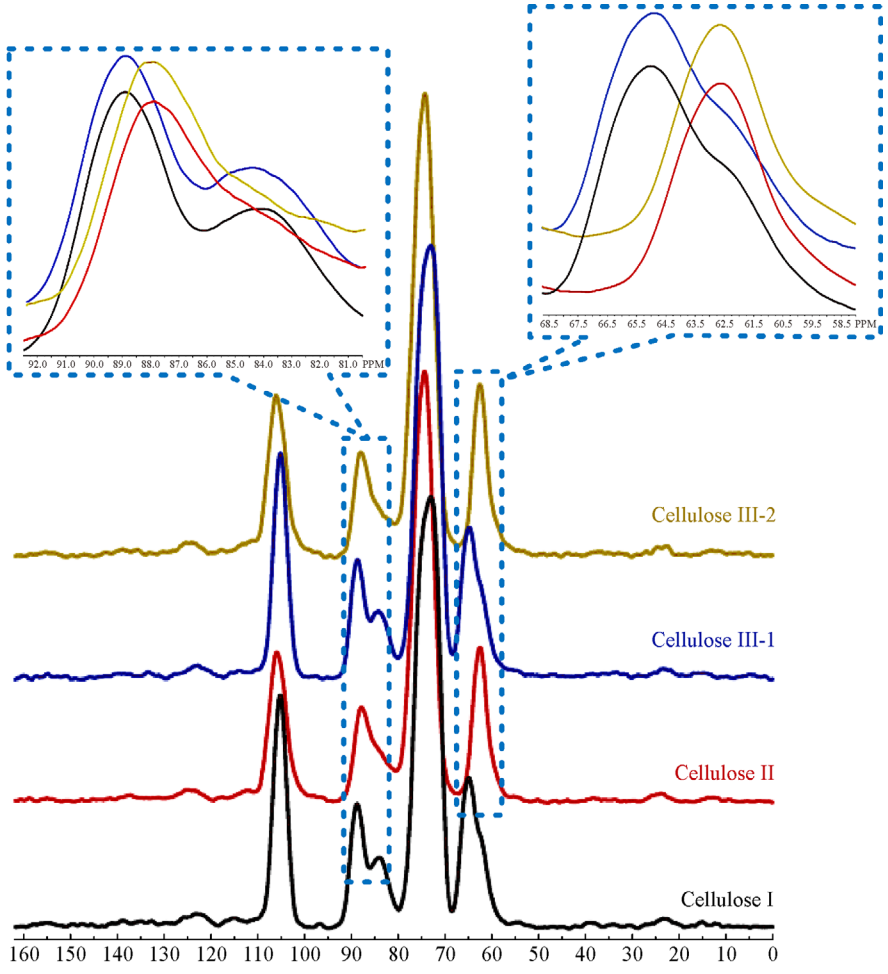

Fig. 2 CP/MAS ^{13}C NMR spectra of cellulose samples

I to the g-t conformation in cellulose II, as well as the simultaneous generation of intra-molecular hydrogen bonds (O_6–H···O_2) (Isogai et al., 1989). Cai and Zhang compared the CP/MAS ^{13}C NMR spectra of cellulose in LiOH (4.2%)/urea (12%)/D_2O and NaOH (7%)/urea (12%)/D_2O and found that the carbonyl carbon had nearly the same chemical shift in the two solution systems, indicating similar interactions between NaOH or LiOH and urea (Cai et al., 2008). However, the intramolecular and intermolecular hydrogen bonds of cellulose in the NaOH/D_2O solution were relatively stronger than those in the LiOH/D_2O solution, resulting in the chemical shifts of carbon to a higher magnetic field (Cai et al., 2006). By simultaneous real-time monitoring, cellulose was seen to swell after 20 s dissolution, was partially dissolved and converted to cellulose II at around 30 s, and completely dissolved after 20 min of treatment. The structural changes of cellulose I can thus be summarized as follows: cellulose I was initially converted to amorphous cellulose and then to cellulose II (Jin et al., 2007).

Due to the high solubility of cellulose in the NaOH/urea system, a liquid-state NMR analysis was applied to examine the structural variation of cellulose, taking NaOD/Urea/D_2O (7/12/81 by weight) as the solvent. According to previous work (Mori et al., 2012; Idström et al., 2016; Wang et al., 2016) and the HSQC NMR spectra (Fig. 3, right), the signals in the ^1H NMR spectra of cellulose polymorphs were identified as: H_4 (2.9 ppm), H_2, H_3, and H_5 (3.0 to 3.3 ppm), H_{6b} (3.4 ppm), H_{6a} (3.5 ppm), and H_1 (4.1 ppm) (Fig. 3, left). Other small signals present in the spectra are ascribed to the C–H protons at the non-reducing or reducing ends of the cellulose chains. Clearly, no obvious difference was found in any sample, since the cellulose chains in any crystal configuration can be dissociated by extensively breaking the hydrogen bonds in NaOH/urea system. Furthermore, the degrees of dissociation C_2–OH, C_3–OH, and C_6–OH can be roughly equal. However, the clear differences in the chemical shifts of C_1 and C_4 between solid and liquid NMR spectra indicate that some conformational variations in the cellulose chains occurred during the dissolving process. Particularly for the cellulose III-1 and -2 samples, the splitting peaks of H_6 were likely a product of the spin-spin coupling of the two adjacent protons at the C_6 position, which were fully released into the solvent. Although alcoholic hydroxyl groups do not completely dissociate and form stable alcoholates in aqueous alkaline solutions, partially dissociated structures of relatively short duration were likely generated. This conclusion is based on the fact that cellulose hydroxyl groups are etherified by SN_2 reactions in aqueous NaOH solutions when preparing methyl-, ethyl-, and carboxymethyl-celluloses (Isogai, 1997). In addition, the degree of C_3–OH dissociation can be related to the driving force of cellulose mercerization under alkaline conditions, which is resisted by intramolecular hydrogen bonding between the oxygen atom of the adjacent glucose and C3–OH. The ^1H NMR spectrum of C–H in cellulose in NaOH (7%)/urea (12%)/D_2O solution was very similar to that of the NaOH/D_2O solution, and the position changes of the C–H peak were similar to that of 20%–24% NaOH. These results show that the cellulose chain was surrounded by NaOH hydrate, and the urea hydrate was outside the sheath of the cellulose and NaOH (Cai et al., 2008).

4 Conclusions

Different crystal configurations of cellulose were successfully prepared and fully characterized using thermal and NMR technologies. The endothermic activity was closely related to the energy consumption required to break the crystalline domains of cellulose. However, cellulose II exhibited the poorest thermal stability and unique

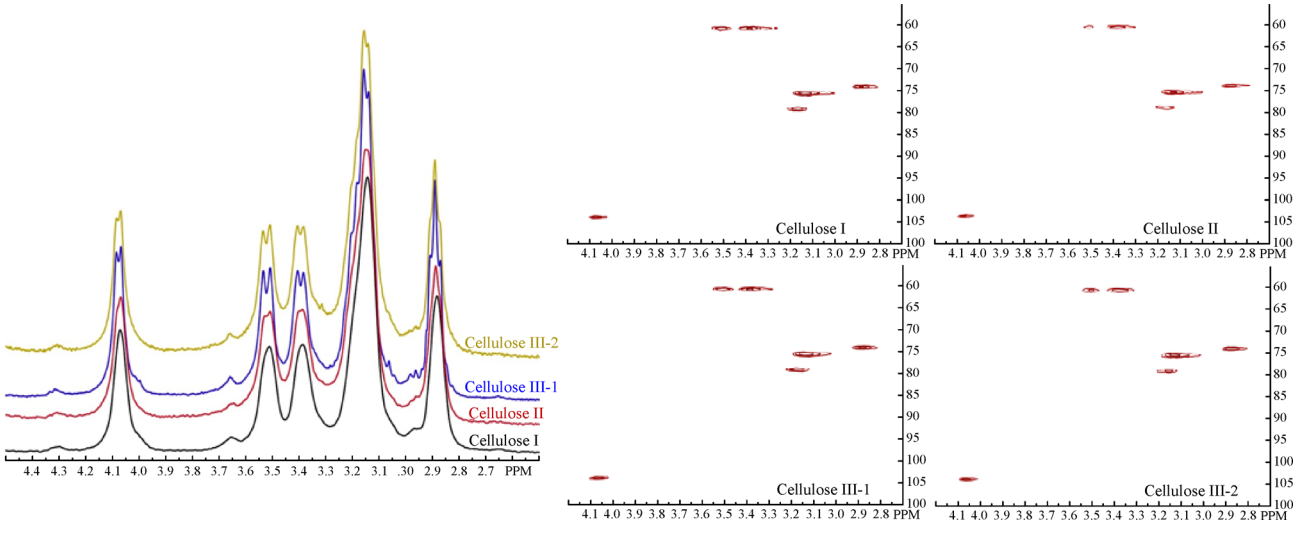

Fig. 3 ^1H (left) and HSQC (right) NMR of cellulose samples

exothermic behavior, which was closely related to its crystal configuration and corresponding low crystallinity. Due to the high cellulose solubility in the NaOH/urea system, the liquid-state NMR analysis with NaOD/Urea/D_2O solvent was employed to examine the structural variation of cellulose. Although no significant difference was found among the samples, clear differences in the chemical shifts of C_1 and C_4 between solid and liquid NMR spectra indicate that conformational variations in the cellulose chains occurred during dissolution. The chemical shift in NMR analysis and thermal behavior reported in this work offer a foundation for future studies of cellulose-based polymers.

References

Ashraf M T, Thomsen M H, Schmidt J E (2017). Hydrothermal pretreatment and enzymatic hydrolysis of mixed green and woody lignocellulosics from arid regions. Bioresource Technology, 238: 369–378

Balat M (2008). Mechanisms of thermochemical biomass conversion processes. Part 1: Reactions of pyrolysis. Energy Sources. Part A, Recovery, Utilization, and Environmental Effects, 30(7): 620–635

Bertran M S, Dale B E (1986). Determination of cellulose accessibility by differential scanning calorimetry. Journal of Applied Polymer Science, 32(3): 4241–4253

Cai J, Liu Y, Zhang L (2006). Dilute solution properties of cellulose in LiOH/urea aqueous system. Journal of Polymer Science. Part B, Polymer Physics, 44(21): 3093–3101

Cai J, Zhang L N, Liu S L, Liu Y T, Xu X J, Chen X M, Chu B, Guo X L, Xu J, Cheng H, Han C C, Kuga S (2008). Dynamic self-assembly induced rapid dissolution of cellulose at low temperatures. Macromolecules, 41(23): 9345–9351

Cai J, Zhang L N, Zhou J P, Li H, Chen H, Jin H M (2004). Novel fibers prepared from cellulose in NaOH/urea aqueous solution. Macromolecular Rapid Communications, 25(17): 1558–1562

Chen J H, Wang K, Xu F, Sun R C (2014). Progress of preparing regenerated cellulose fibers using novel dissolution process. CIESC Journal, 65: 4213–4221

Chen X, Chen J, You T, Wang K, Xu F (2015). Effects of polymorphs on dissolution of cellulose in NaOH/urea aqueous solution. Carbohydrate Polymers, 125: 85–91

Chen X M, Burger C, Fang D F, Ruan D, Zhang L N, Hsiao B S, Chu B (2006). X-ray studies of regenerated cellulose fibers wet spun from cotton linter pulp in NaOH/thiourea aqueous solutions. Polymer, 47 (8): 2839–2848

Cheng G, Varanasi P, Li C, Liu H, Melnichenko Y B, Simmons B A, Kent M S, Singh S (2011). Transition of cellulose crystalline structure and surface morphology of biomass as a function of ionic liquid pretreatment and its relation to enzymatic hydrolysis. Biomacromolecules, 12(4): 933–941

Egal M, Budtova T, Navard P (2008). The dissolution of microcrystalline cellulose in sodium hydroxide-urea aqueous solutions. Cellulose (London, England), 15(3): 361–370

Himmel M E, Ding S Y, Johnson D K, Adney W S, Nimlos M R, Brady J W, Foust T D (2007). Biomass recalcitrance: Engineering plants and enzymes for biofuels production. Science, 315(5813): 804–807

Huang H, Liu Y, Chao M A, Jiyou G U (2016). Research progress in the application of cellulose and its derivatives. Materials Review, 21: 75–82

Idström A, Schantz S, Sundberg J, Chmelka B F, Gatenholm P, Nordstierna L (2016). (^{13})C NMR assignments of regenerated cellulose from solid-state 2D NMR spectroscopy. Carbohydrate Polymers, 151: 480–487

Ishikawa A, Okano T, Sugiyama J (1997). Fine structure and tensile properties of ramie fibres in the crystalline form of cellulose I, II, III_I and IV_I. Polymer, 38(2): 463–468

Isogai A (1997). NMR analysis of cellulose dissolved in aqueous NaOH solutions. Cellulose (London, England), 4(2): 99–107

Isogai A, Usuda M, Kato T, Uryu T, Atalla R H (1989). Solid-state CP/MAS carbon-13 NMR study of cellulose polymorphs. Macromolecules, 22(7): 3168–3172

Jeoh T, Ishizawa C I, Davis M F, Himmel M E, Adney W S, Johnson D K (2007). Cellulase digestibility of pretreated biomass is limited by cellulose accessibility. Biotechnology and Bioengineering, 98(1): 112–122

Jin F, Zhang J, Chen W, Fan Q, Bai Z (2012). Preparation and chiral recognition of new chiral stationary phases derived from cellulose microspheres. Wuhan University Journal of Natural Sciences, 17(3): 205–210

Jin H, Zha C, Gu L (2007). Direct dissolution of cellulose in NaOH/thiourea/urea aqueous solution. Carbohydrate Research, 342(6): 851–858

Junior J L P (2000). Effect of cellulose crystallinity on the progress of thermal oxidative degradation of paper. Journal of Applied Polymer Science, 78: 61–66

Kono H, Erata T, Takai M (2003). Complete assignment of the CP/MAS ^{13}C NMR spectrum of cellulose III_I. Macromolecules, 36(10): 3589–3592

Kumar P, Barrett D M, Delwiche M J, Stroeve P (2009). Methods for pretreatment of lignocellulosic biomass for efficient hydrolysis and biofuel production. Industrial & Engineering Chemistry Research, 48 (8): 3713–3729

Langan P, Nishiyama Y, Chanzy H (1999). A revised structure and hydrogen-bonding system in cellulose II from a neutron fiber diffraction analysis. Journal of the American Chemical Society, 121 (43): 9940–9946

Lennholm H, Larsson T, Iversen T (1994). Determination of cellulose I [alpha] and I[beta] in lignocellulosic materials. Carbohydrate Research, 261(1): 119–131

Liebert T, Heinze T, Edgar K J (2010). Cellulose solvents: For analysis, shaping and chemical modification. Journal of the American Chemical Society, 132: 17976–17976

Liitiä T, Maunu S L, Hortling B, Tamminen T, Pekkala O, Varhimo A (2003). Cellulose crystallinity and ordering of hemicelluloses in pine and birch pulps as revealed by solid-state NMR spectroscopic methods. Cellulose (London, England), 10(4): 307–316

Lou Y R, Kanninen L, Kuisma T, Niklander J, Noon L A, Burks D, Urtti A, Yliperttula M (2014). The use of nanofibrillar cellulose hydrogel

as a flexible three-dimensional model to culture human pluripotent stem cells. Stem Cells and Development, 23(4): 380–392

Luo X, Zhang L (2010). Immobilization of penicillin G acylase in epoxy-activated magnetic cellulose microspheres for improvement of biocatalytic stability and activities. Biomacromolecules, 11(11): 2896–2903

Madaeni S S, Heidary F (2011). Improving separation capability of regenerated cellulose ultrafiltration membrane by surface modification. Applied Surface Science, 257(11): 4870–4876

Moigne N L, Navard P (2010). Dissolution mechanisms of wood cellulose fibres in NaOH–water. Cellulose (London, England), 17(1): 31–45

Mori T, Chikayama E, Tsuboi Y, Ishida N, Shisa N, Noritake Y, Moriya S, Kikuchi J (2012). Exploring the conformational space of amorphous cellulose using NMR chemical shifts. Carbohydrate Polymers, 90(3): 1197–1203

Mosier N, Wyman C, Dale B, Elander R, Lee Y Y, Holtzapple M, Ladisch M (2005). Features of promising technologies for pretreatment of lignocellulosic biomass. Bioresource Technology, 96(6): 673–686

Nishino T, Matsuda I, Hirao K (2004). All-cellulose composite. Macromolecules, 37(20): 7683–7687

Perlack R D, Wright L L, Turhollow A F, Graham R L, Stokes B J, Erbach D C (2005). Biomass as feedstock for a bioenergy and bioproducts industry: The technical feasibility of a billion-ton annual supply. Oak Ridge National Lab TN, doi: 10.2172/885984

Qin X, Lu A, Cai J, Zhang L (2013a). Stability of inclusion complex formed by cellulose in NaOH/urea aqueous solution at low temperature. Carbohydrate Polymers, 92(2): 1315–1320

Qin X, Lu A, Zhang L (2013b). Gelation behavior of cellulose in NaOH/urea aqueous system via cross-linking. Cellulose (London, England), 20(4): 1669–1677

Sarko A (1978). What is the crystalline structure of cellulose? Technical Association of the Pulp and Paper Industry, Tappi

Segal L, Creely J J, Martin A E Jr, Conrad C M (1959). An empirical method for estimating the degree of crystallinity of native cellulose using the X-ray diffractometer. Textile Research Journal, 29(10): 786–794

Teng N, Ni J, Chen H Z, Ren Q H, Na H N, Liu X Q, Zhang R Y, Zhu J (2016). Initiating highly effective hydrolysis of regenerated cellulose by controlling transition of crystal form with sulfolane under microwave radiation. ACS Sustainable Chemistry & Engineering, 4 (3): 1507–1511

Tsarevsky N V, Bernaerts K, Dufour B, Prez F D, Matyjaszewski K (2004). Well-defined (Co) polymers with 5-vinyltetrazole units via combination of atom transfer radical (Co) polymerization of acrylonitrile and “click chemistry”-type postpolymerization modification. Macromolecules, 37(25): 9308–9313

Wang J, Lin X, Luo X, Yao W (2015). Preparation and characterization of the linked lanthanum carboxymethylcellulose microsphere adsorbent for removal of fluoride from aqueous solutions. RSC Advances, 5(73): 59273–59285

Wang L H, Wang Y L, Zhao X S, Han Z (2013). Comparative study on the method of extracting straw cellulose. Zhongguo Nongxue Tongbao, 29: 130–134 (in Chinese)

Wang T, Phyo P, Hong M (2016). Multidimensional solid-state NMR spectroscopy of plant cell walls. Solid State Nuclear Magnetic Resonance, 78: 56–63

Wang Y, Deng Y (2009). The kinetics of cellulose dissolution in sodium hydroxide solution at low temperatures. Biotechnology and Bioengineering, 102(5): 1398–1405

Yang B, Wyman C E (2008). Pretreatment: The key to unlocking low-cost cellulosic ethanol. Biofuels, Bioproducts & Biorefining, 2(1): 26–40

Yui T, Okayama N, Hayashi S (2010). Structure conversions of cellulose III_I crystal models in solution state: A molecular dynamics study. Cellulose (London, England), 17(4): 679–691

Zhang J Q, Lin L, Sun Y, Mitchell G, Liu S J (2008). Advance of studies on structure and decrystallization of cellulose. Linchan Huaxue Yu Gongye, 28: 109–114 (in Chinese)